A Two-Level Integrated Optimization System for Planning of Emergency Evacuation

Ying Liu[1], Xiaorong Lai[2], and Gang-len Chang, M.ASCE[3]

ABSTRACT: This paper presents a two-level integrated optimization system for use in generating the candidate set of optimal evacuation plans that serve as the input for simulation-based evacuation systems. In the proposed system, the high-level optimization aims to maximize the throughput during the specified evacuation duration, and the low level intends to minimize the total travel time as well as waiting time for the entire operation if the specified duration is sufficient for evacuating all demands. To effectively represent traffic flow relations with mathematical formulations, this paper employs the cell transmission concept, but with a revised formulation for large-scale network applications. The performance of the proposed models and their applicability has been tested with a microscopic simulation program that replicates the Ocean City evacuation network. Evaluation results from these numerical studies have demonstrated the promising properties of the proposed integrated optimization system.

CE Database subject headings: Evacuation; Planning; Optimization models; Hurricanes

Introduction

Modern cities are exposed to various potential disasters, including not only the natural hazards such as hurricanes, but also technological and terrorist-induced emergencies such as nuclear leakage and biohazard attacks (Urbina and

Wolshon 2003; Demuth 2002). The potential severity level is often compounded by the concentration of population and congestion of available transportation networks (Alsnih and Stopher 2003). Thus, how to effectively contend with emergency evacuation related issues has emerged as one of the utmost tasks for both the research community and responsible agencies.

In review of the related literature, it is noticeable that a variety of studies for different evacuation needs have been conducted, and some operational systems have also been developed. For example, NETVACI, one of the earliest evacuation planning tools developed in the 1980's, can simulate the evacuation process based on mathematical relationships between flows, speeds, densities, queue length and other important traffic parameters (Sheffi et al. 1982). At the same macroscopic level, MASSVAC and its successors (MASSVAC 3.0, MASSVAC 4.0 and TEDSS) developed in the 80's and 90's employ static traffic assignment models to project the flow distribution during evacuation (Hobeika et al. 1985; 1994; 1998). From the mid 1980's, microscopic simulators emerged as a widely used tool for evacuation planning. Examples of such systems include CEMPS, IMDAS, OREMS and other practices (Pidd et al. 1996; Franzese and Han 2001; ORNL 2002; Jha et al. 2004; Theodoulou and Wolshon 2004; Zou and Yeh 2005).

Although simulation has been proved to be an efficient tool for design and evaluation of evacuation plans, its generation of a final solution is often limited by the available candidate plans. In practice, these candidate plans are usually proposed based on the experience of responsible practitioners, which could deviate far from the optimal control plan and consequently demand a tremendous amount of simulation time as well as efforts to finalize necessary adjustments. To circumvent such limitations, this paper presents a two-level integrated optimization

system that intends to yield the range of most viable parameters for target control strategies, such as the percentage

of demands to be diverted to each evacuation route and turning fractions to be regulated at critical junctions. Based

on mathematically formulated traffic flow relations and operational constraints, the optimization system is capable

of identifying the candidate set of optimal evacuation plans in a timely manner even for large networks.

Responsible system users can then finalize the control plans with a pre-calibrated simulator that can realistically

replicate some critical operational features and driver response difficult to be fully captured with analytical

formulations (e.g., turning bay length or merging behavior). Thus, the primary purpose of the proposed optimization

system is to efficiently and effectively provide candidate evacuation plans and consequently improve efficiency of

evacuation planning and operations.

The remaining of this paper is organized as follows. To efficiently model the dynamic nature of the evacuation

traffic, next section proposes a revised cell transmission formulation specially designed for large-scale network

applications. Then, Section 3 will detail the formulations for the optimization models. Section 4 illustrates the

evaluation results with respect to the system performance and its applicability in a real-world network. Section 5

summarizes research findings and potential applications of the proposed optimization models.

The Underlying Network Flow Formulation

To ensure the effectiveness of the proposed optimization models, one has to choose an approach to mathematically

represent traffic flow evolution in an evacuation highway network. A variety of methods have been proposed in the

literature. For example, Barrett et al. (2000) have developed a dynamic traffic management framework for hurricane

evacuations based on dynamic traffic assignment. Following the practice of Ziliaskopoulos, et al. (1999; 2000),

Tuydes and Ziliaskopoulos (2000) employed the cell transmission model for evacuation planning. To accommodate the complexity associated with large-scale network applications and to improve the computational efficiency, this study proposes a revised cell transmission formulation for use as the underlying network flow model.

The basic idea of the cell transmission concept proposed by Daganzo (1994; 1995) is to convert highway links into equal-sized segments, or called cells, that could be traversed in a unit time interval at the free-flow speed. Then, the movements of vehicles among these cells are defined with two types of relations, namely flow propagation relations to decide flows between two cells based on upstream/downstream traffic conditions and flow conservation equations to depict the evolution of the cell status (i.e., the number of vehicles in each cell) over time.

To reduce the size of formulations in large-scale network applications, Ziliaskopoulos and Lee (1996) have proposed the use of cells of adjustable size. Their idea is to update those longer cells with a lower frequency, and use the averaged parameters for those intermediate intervals. Such a formulation requires the size of a long cell to be an integral multiple of its connected short cells, and may cause the propagated flows deviated from those with homogenous cells.

To offer the flexibility and also to improve model accuracy in large-scale network applications, the revised cell transmission formulation proposed in this study will allow cells of different sizes to be connected arbitrarily. Its core concept is presented below.

Network Conversion

To successfully apply the revised cell transmission formulation, one needs to convert the highway network into a set

of connected cells following the principal steps summarized below:

- **Identify homogenous road segments**: homogeneity is defined by the same free flow speed, same number

  of lanes, same jam density, same saturation flow rate, and no ramps within a segment.

- **Define unit time interval**: the maximal unit interval τ is constrained by the shortest time to traverse a

  homogenous segment, as in Equation 1. Other unit intervals can also be used, provided τ is the integral

  multiple of it.

$$\tau = \min\{\frac{length \quad of \quad a \quad segment}{corresponding \quad free \quad flow \quad speed}\}$$ 1)

- **Convert road segments to cells**: basically, every homogenous segment is converted to a cell, and the cell

  size l is defined by Equation 2.

$$l = \frac{length \quad of \quad segment}{corresponding \quad free \quad flow \quad speed \times unit \quad interval \quad length}$$ 2)

- **Define connectors between cells**: A connector is defined to indicate the potential traffic flows between

  two connected segments.

Flow Conservation Formulation

Flow conservation equations depict the evolution of the cell status (i.e., the number of vehicles in each cell) over

time. With the revised cell transmission formulation, all cells will be updated at every unit time interval τ

regardless of their size. As illustrated in Figure 1, Equation 3 and Equation 4 define the flow conservation relations

for different types of cells.

For general cells (actual highway segments) and sink cells (destinations),

$$x_i^{t+1} = x_i^t + \sum_{k \in \Gamma^{-1}(i)} y_{ki}^t - \sum_{j \in \Gamma(i)} y_{ij}^t \qquad \text{3)}$$

For source cells (origins),

$$x_r^{t+1} = x_r^t + d_r^t - \sum_{j \in \Gamma(r)} y_{rj}^t \qquad \text{4)}$$

x_i^t = the number of vehicles in cell i at the beginning of interval t ; y_{ij}^t = connector flows from cell i to cell j

during t ; d_r^t = evacuation demand from origin r during interval t , which is also called dynamic loading pattern

and defined with response curves in practice; $\Gamma(i)$ = the set of downstream cells to cell i ; $\Gamma^{-1}(i)$ = the set of

upstream cells to cell i ; The subscript r = index of source cells; i, j, k = index of other cells.

Revised Flow Propagation Formulation

The flow propagation relations decide the connecting flows between cells during each time interval, which are

presented with the following expressions:

$$\sum_{k \in \Gamma^{-1}(i)} y_{ki}^t \leq R_i^t \qquad \text{5)}$$

$$\sum_{j \in \Gamma(i)} y_{ij}^t \leq S_i^t \qquad \text{6)}$$

Equation 5 is to model flow propagation relations considering the traffic conditions in a downstream cell, whereas

Equation 6 is for the traffic conditions in an upstream cell. R_i^t = receiving capacity of downstream cell i during

interval t (veh); S_i^t = sending capability of upstream cell i during interval t (veh);

Equation 7 defines the receiving capacity of cell i , which is proposed after considering the initial cell status x_i^t as

well as its potential *internal* evolution during interval t . The mathematical proof is shown in the Appendix.

$$R_i^t = \min \{Q_i^t, N_i^t / l_i, N_i^t - x_i^t\} \qquad \text{7)}$$

Q_i^t = number of vehicles that can flow into/out of cell i during t ; N_i^t = number of vehicles that can present in cell i during t ; l_i = size of cell i . Note that if the cell length l_i is equal to 1, Equation 7 will converge to the equation for equal-sized cells in the classic cell transmission formulation.

Equation 8 defines the sending capacity of cell i . Note that if l_i is equal to 1, Equation 8 is also equivalent to the equation for equal-sized cells (Daganzo 1994).

$$S_i^t = \min\{Q_i^t, \; N_i^t / l_i, \; x_i^{t-l_i+1} - \sum_{j\in\Gamma(i)} \sum_{m=t-l_i+1}^{t-1} y_{ij}^m \} \qquad\qquad 8)$$

The first two terms are direct presentation of the maximal flow that can leave cell i during a unit time interval. The third term can be explained as follows: according to the definition of cell size, l_i unit intervals are required to traverse cell i at the free-flow speed. Thus, the total flows that should have left cell i are $\sum_{k\in\Gamma^{-1}(i)} \sum_{m=1}^{t-li} y_{ki}^m$, while the total flows that have actually left cell i are $\sum_{j\in\Gamma(i)} \sum_{m=1}^{t-1} y_{ij}^m$. The sending capacity cannot exceed their difference, i.e.,

$$S_i^t \le \sum_{k\in\Gamma^{-1}(i)} \sum_{m=1}^{t-li} y_{ki}^m - \sum_{j\in\Gamma(i)} \sum_{m=1}^{t-1} y_{ij}^m = x_i^{t-li+1} - \sum_{j\in\Gamma(i)} \sum_{m=t-li+1}^{t-1} y_{ij}^m \qquad\qquad 9)$$

Formulation of the Optimization Models

Applying the revised cell transmission concept as the underlying network flow model, this section will detail the model formulations for the proposed optimization system.

Objective Functions

In response to the unique operational constraints during emergency evacuation, the proposed optimization system features a two-level optimization scheme.

The high-level optimization aims to maximize the total throughput within the specified evacuation duration T. Since the throughput can be represented with the total number of vehicles entering all destinations over the study period, one can formulate the objective function as follows:

$$\max \quad \sum_{s \in Cs} \sum_{i \in \Gamma^{-1}(s)} \sum_{t=1}^{T} y_{is}^{t} = \sum_{s} x_{s}^{T+1} \qquad\qquad 10)$$

C_S = the set of sink cells (destinations); the subscript s = index of sink cells.

The low-level optimization model intends to minimize the total trip time (including the waiting time in origins) if the specified duration is sufficient for evacuating all demands. The special structure of the underlying network flow model implies that a vehicle in a cell will either wait for one interval without move or take one interval to reach the downstream cell. Thus, the objective function has the following expression:

$$\min \quad \sum_{i \in C \cup Cr} \sum_{t=1}^{T+1} x_{i}^{t} \qquad\qquad 11)$$

C = the set of general cells (highway segment); C_r = the set of source cells (origins)

Network Flow Constraints

Applying the revised cell transmission formulation, one can summarize the network flow constraints for both levels of optimization as below.

$$x_{i}^{t+1} = x_{i}^{t} + \sum_{k \in \Gamma^{-1}(i)} y_{ki}^{t} - \sum_{j \in \Gamma(i)} y_{ij}^{t}, \qquad i \in C \cup C_s \qquad\qquad 12)$$

$$x_{r}^{t+1} = x_{r}^{t} + d_{r}^{t} - \sum_{j \in \Gamma(r)} y_{rj}^{t}, \qquad r \in C_r \qquad\qquad 13)$$

$$\sum_{k\in\Gamma^{-1}(i)} y_{ki}^t \le Q_i^t, \qquad i\in C\cup C_s \tag{14}$$

$$\sum_{k\in\Gamma^{-1}(i)} y_{ki}^t \le N_i^t / l_i, \qquad i\in C\cup C_s \tag{15}$$

$$\sum_{k\in\Gamma^{-1}(i)} y_{ki}^t \le N_i^t - x_i^t, \qquad i\in C\cup C_s \tag{16}$$

$$\sum_{j\in\Gamma(i)} y_{ij}^t \le Q_i^t, \qquad i\in C \tag{17}$$

$$\sum_{j\in\Gamma(i)} y_{ij}^t \le N_i^t / l_i, \qquad i\in C \tag{18}$$

$$\sum_{j\in\Gamma(i)} y_{ij}^t \le x_i^{t-l_i+1} - \sum_{j\in\Gamma(i)} \sum_{m=t-l_i+1}^{t-1} y_{ij}^m, \qquad i\in C \tag{19}$$

Demand Related Constraints

High Level

At this level, no constraint is enforced on the evacuation demand if there is only one origin, i.e., the connector flows from a source cell to its downstream cells are restricted only by the capacity of the evacuation routes. One does not need the flow conservation equations at the source cell.

Under the scenario of multiple origins for evacuation demands, one needs to set proper constraints to reflect the actual evacuation demand from each origin. Otherwise, some origins may contribute more than their actual demands to the total throughput, while outflows from other origins may remain below their demands. To contend with this issue, one can add a new class of constraints, as shown in Equation 20, to restrict the total outflow from a source cell.

$$\sum_{j\in\Gamma(r)} \sum_{t=1}^{T} y_{rj}^t \le D_r \tag{20}$$

Low Level

At this level, one needs to restrict the total demand of source cells with Equation 21.

$$\sum_{j\in\Gamma(r)}\sum_{t=1}^{T}y_{rj}^{t} = D_r$$ 21)

Note that since evacuation flows are counted in the objective function only before they have arrived at their destinations, the model tends to push vehicles as many as possible at the fastest pace. Thus, one can expect that all evacuation demands can reach their destinations at the end of the evacuation period. Equation 22 is proposed to guarantee such a relation: the left-side term is the total number of vehicles that have arrived at destinations after evacuation duration T and the right-side term denotes the total demand.

$$\sum_{s\in Cs} x_s^{T+1} = \sum_{r\in Cr} D_r$$ 22)

Other General Constraints

The general constraints include nonnegative constraints, initial value of cell state variables x_i^0, and initial value of connector flows y_{ij}^0. In most cases, x_i^0 (excluding source cells) and y_{ij}^0 are set to zero, although x_i^0 can be other values to simulate the background traffic prior to the evacuation. Note that x_i^0 can also be used to reflect the actual network condition preceding the onset of an accident during the evacuation and this enables the model users to adjust evacuation plans as needed.

Another class of general constraints is the capacity of destinations. Storage capacity N_s^t can be restricted if the safety shelter has space limitation. Flow capacity Q_s^t may be restricted if the entrance capacity of the safety shelter is lower than the capacity of the upstream routes, or if the destination is not the safety shelter but a dummy node to

indicate safe area. In the later case, Q_s^t is set as the capacity of downstream routes to prevent the queue spillback. As the important evacuation control strategies, both diverging proportions and merging proportions are directly estimatable from the optimization results.

Numerical Analysis and Applications

This section presents the numerical results for two carefully-designed experimental scenarios. The first aims to test the properties of the revised cell transmission formulations, while the second is to demonstrate the model's applicability with the Ocean City hurricane evacuation network.

Test-1: Effectiveness of the Revised Cell Transmission Formulation

This test intends to compare the performance of the following three network flow formulations:

- − Model 1: original cell transmission model with homogenous cells (Daganzo 1994, 1995);

- − Model 2: Ziliaskopoulos' model with averaging technique for longer cells (Ziliaskopoulos and Lee 1996);

- − Model 3: the revised cell transmission formulation proposed in this study.

A 10 km link of two lanes is built in this test, and its key characteristics are given as: free-flow speed = 60 km per hour, jam density = 106 vehicles per km per lane, and saturation flow rate = 2160 vehicles per hour per lane. The travel demand is randomly generated between 0 ~ 1.5 times of link flow capacity.

Figure 2 shows two different cell connection diagrams for a unit interval of one minute. The first one using equal-sized cells is for Model 1, with $Q_i^t = 36veh$, $N_i^t = 106veh$, i=1, …, 10. The second diagram is for Models 2 and 3,

which combines cells between Cell 2 and Cell 9 in the first diagram to form a long cell. The cell marked with r indicates the origin, whereas the cell marked with s denotes the destination.

Two scenarios are tested here. The first scenario is the normal traffic condition without queues. The second scenario presents an accident in the cell ahead of the destination. The capacity of this cell decreases to $Q_i^t = 10veh$ during the time interval $t=20, \ldots, 40min$ due to the accident. Figure 3 illustrates the cumulative arriving curves at the destination for all three models.

As shown in the graphical results, the proposed Model 3 has nearly the same performance as Model 1 (the original cell transmission formulation), regardless of traffic conditions. However, Model 2 tends to deviate from Model 1 in each scenario. Regarding the computational efficiency, the total number of variables with Model 3, although slightly exceeding that of Model 2, is significantly less than the number of variables with Model 1. The number of cell state variables per time interval decreases from 12 in Model 1 to 5 in Model 3, while the number of connector flows per time interval decreases from 11 in Model 1 to 4 in Model 3. The reduction with respect to the number of variables exceeds 60%. This implies that the proposed revised cell transmission formulations can substantially reduce the size of the entire optimization formulations and the computation time for the solution.

Test-2: Case Study in Ocean City

This case study intends to demonstrate the applicability of the proposed optimization models. Ocean City, a famous tour destination, is a narrow peninsula on Maryland Eastern Shore. The population in the summer peak season can reach 150,000 ~ 300,000 people, compared with 7,000 to 25,000 people during the off-peak season (Ocean City

Emergency Operations Plan, 2002). This large size of population in the summer season renders the city especially

vulnerable to the threat of hurricanes, which demands the state to design its hurricane evacuation plans.

Evacuation Scenario

Figure 4 presents the major evacuation network for Ocean City. The sole origin is set to be the entire city. Thus, one

can divide the city into a number of evacuation zones, based on the optimized demand distribution to the three

primary evacuation routes. Among these routes, US50 is an arterial street with two lanes in each direction, MD90 is

a freeway with one lane in each direction, and DE20 is an arterial street with one lane in each direction.

Note that as indicated in the widely adopted evacuation response curves (Alsnih and Stopher 2003), the evacuation

demand from origin r in time interval t, d_r^t, tends to greatly exceed the evacuation capacity after the inception of

evacuation, and the evacuation demand will accumulate in the source cells until the final dissipation phase. Thus,

this paper assumes that all traffic demand can enter their corresponding source cell before the first time interval.

Such an assumption will not affect the resulting throughput and the total travel time under the optimized evacuation

plan.

There are three destinations for evacuation flows. The city of Salisbury is a destination without capacity limit, while

US113 north and US113 south are two dummy destinations with a flow capacity of 1800 vehicle per lane per hour.

Network Conversion

Following the network conversion procedures in Section 2, this paper first defines the homogenous segments. Note that all interchanges are modeled with connectors, not cells, to indicate the existence of ramps. The jam density for all cells is set to be 93 vehicles per kilometer per lane, whereas the saturation flow rate is set to be 2160 vehicles per lane per hour for the freeway segment of MD90, and 1800 vehicles per lane per hour for other segments. Based on the actual network geometric data, the length of a unit interval is set to be 20 seconds, which is sufficiently small for evacuation operations. Then, one can convert the network to a cell connection diagram as illustrated in Figure 5. Note that the number in each parenthesis indicates the size of the cell.

High-Level Optimization: To Maximize the Throughput

With the proposed formulations, this section intends to show the function of the proposed high-level optimization model for maximizing the total throughput during the given evacuation duration.

In this application, the LP formulations contain 720 time intervals, 79,809 variables, and 250,509 constraints. A computer program was created to generate the standard input file for the professional software LINGO 8.0. The global optimal solution for the maximal throughput over the evacuation period of 4 hours amounts to 27,268 vehicles to all three destinations. Figure 6 presents the cumulative arriving curve for each destination, where most vehicles are directed to Salisbury.

Low-Level Optimization: To Minimize the Total Travel Time and Waiting Time

The application in this section is to explore the function of the proposed low-level optimization model in optimizing

the evacuation patterns if the allowed time window is sufficiently long for completing the evacuation. The total

evacuation demand is set to be 25,000 vehicles in 4 hours. The new LP formulations with the second level

optimization contain 80,528 variables and 251,228 constraints for 720 time intervals. Figure 7 presents the

cumulative arriving curve of each destination based on the global optimal solution.

The preliminary results from the low-level model indicate that there is no flow in the south direction of US113

between US50 and MD90, and the capacity usage of the north direction of US113 from US50 to DE54 is very low.

Thus, one can exclude these road segments from the major evacuation network in practice. Note that after excluding

those low-usage routes, only two diverging cells and one merging cells remain in the network, where

- − Cell 6 is a diverging cell: The connector from Cell 6 to Cell 7 carries the through traffic on US50, while the

    connector from Cell 6 to Cell 40 conveys the traffic from US50 to US113 South;

- − Cell 7 is a diverging cell: The connector from Cell 7 to Cell 8 carries the through traffic on US50, while the

    connector from Cell 7 to Cell 24 conveys the traffic from US 50 to MD346;

- − Cell 9 is a merging cell: The connector from Cell 8 to Cell 9 captures the through traffic on US50, while

    the connector from Cell 16 to Cell 9 carries the traffic from MD90 to US50.

Analysis of the flow proportions in those critical points indicates that their diverging/merging patterns are relatively

stable, except during the dissipation phase.

- For the merging Cell 9, the proportion between the through traffic on US 50 and merging traffic from MD 90 always keeps at the ratio of 0.4 versus 0.6.

- For diverging Cell 6, through traffic on US 50 and turning traffic from US50 to US113 south has maintained the ratio of 1:1 during the first 581 intervals (approximately 3 hr 14 min). During the subsequent 26 intervals (approximately 9 min), the optimal turning proportion tends to vary significantly. During the remaining intervals (approximately 37 min), all traffic arriving at this diverging point should go to US113 south.

- For diverging Cell 7, through traffic on US50 and turning traffic from US50 to MD346 will keep the ratio of 0.8 versus 0.2 during the first 588 intervals (approximately 3 hr 16 min). For the remaining intervals (approximately 44 min), all traffic arriving at this diverging point will go to US50.

Simulation Comparison of the Proposed Network Flow Formulations

Finally, this section intends to evaluate the effectiveness and reliability of the proposed formulations for application in the Ocean City network. For this purpose, one can compare the cumulative arriving curve at each destination generated from the model with the same curves generated from the network simulator developed with CORSIM.

Note that the optimal turning fractions from the low-level optimization may vary significantly over some periods in the ideal case, which are not suitable for direct use as simulation input and not realistic for real-world implementation. To reflect this operational constraint, the diverging proportions for Cells 6 and 7 are set as those shown in Table 1, based on the low-level optimization results.

Note that the diverging flow rates for the connector between Cell 6 and Cell 40 (US 50 to US 113 south) is quite high for the actual ramp capacity. Some controls will be needed to ensure that traffic congestion will not occur on the upstream links to Cell 6. Hence, the node from US50 to US113 south has been operated with the following plans.

- − Extending deceleration lane to US113 south till its upstream off ramp to US113 north

- − Using the shoulder of the weaving lane as a turning pocket.

- − Converting one shoulder as one additional ramp lane.

Figure 8 presents the comparison results, which indicate that the time-varying network traffic conditions generated with the revised cell transmission formulation are quite similar to those obtained from the microscopic simulator. This indicates the potential of the proposed model in accurately formulating traffic flows for large-scale networks and in efficiently generating the optimal set of evacuation strategies for real-time operations.

Conclusions

This paper has presented a two-level optimization system for large-scale network evacuation planning, which is capable of efficiently providing the candidate set of optimal evacuation plans for review by responsible experts and/or for refinement with various network simulators. To efficiently model the flow propagation in large-scale networks, this study has proposed a revised cell-transmission formulation as its underlying network flow model, which has proved to yield sufficiently reliable performance. The applicability of the proposed two-level optimization system and its reliability for use in practice has also been evaluated with the Ocean City network simulator.

Overall, despite the difficulty in capturing all operational constraints with analytical formulations, the proposed optimization system can effectively and efficiently generate a set of optimal emergency evacuation plans under available resources and the evacuation time window. Such a capability in identifying promising plans is critical in real-time evacuation operations, especially when the traffic flows encounter unexpected events during the evacuation and the revised control strategies needs to be generated in a timely manner.

Appendix

Proof: First, one can divide the long cell i into l_i homogenous sub-cells of size 1, which can be traversed in a unit time interval at free flow speed. Define sx_k^t = the number of vehicles on sub-cell k at the beginning of interval t; Ω_k^t = the flow that can be sent from sub-cell k to sub-cell $k+1$ during t; Ψ_k^t = the surplus flow on sub-cell k after sending Ω_k^t to sub-cell $k+1$.

If $Q_i^t \geq N_i^t / l_i$, one can find the following iteration relations:

$$\Omega_{li-1}^t = \min\{N_i^t / l_i - sx_{li}^t, sx_{li-1}^t\} \Rightarrow \Psi_{li-1}^t = \max\{sx_{li-1}^t + sx_{li}^t - N_i^t / l_i, \ 0\}$$

$$\Omega_k^t = \min\{N_i^t / l_i - \Psi_{k+1}^t, sx_k^t\} \Rightarrow \Psi_k^t = \max\{sx_k^t + \Psi_{k+1}^t - N_i^t / l_i, \ 0\}, k = 1, \ldots, l_i - 2$$

Substituting Ψ_2^t into the equation of Ψ_1^t and considering $\sum_{k=1}^i sx_k^t \leq iN_i^t / l_i$, one can have

$$\Psi_1^t = \max\{sx_1^t + sx_2^t + \Psi_3^t - 2N_i^t / l_i, \ 0, \ sx_1^t - N_i^t / l_i\} = \max\{sx_1^t + sx_2^t + \Psi_3^t - 2N_i^t / l_i, \ 0\}$$

Then by substituting $\Psi_3^t, \ldots, \Psi_{li-1}^t$ one by one, one can finally have

$$\Psi_1^t = \max\{\sum_k sx_k^t - (l_i - 1)N_i^t / l_i, \ 0\} = \max\{x_i^t - (l_i - 1)N_i^t / l_i, \ 0\}$$

Thus the vacant in sub-cell 1, namely the receiving capacity of cell i is given by

$$R_i^t = N_i^t / l_i - \Psi_1^t = \min\{N_i^t - x_i^t, \ N_i^t / l_i\} = \min\{N_i^t - x_i^t, \ N_i^t / l_i, \ Q_i^t\}$$

If $Q_i^t < N_i^t / l_i$, one can find a more complex iteration relations:

$$\Omega_{li-1}^t = \min\{N_i^t / l_i - sx_{li}^t, sx_{li-1}^t, Q_i^t\} \Rightarrow \Psi_{li-1}^t = \max\{0, sx_{li-1}^t - Q_i^t, sx_{li}^t + sx_{li-1}^t - N_i^t / l_i\}$$

$$\Omega_k^t = \min\{N_i^t / l_i - \Psi_{k+1}^t, sx_k^t, Q_i^t\} \Rightarrow \Psi_k^t = \max\{0, sx_k^t - Q_i^t, \Psi_{k+1}^t + sx_k^t - N_i^t / l_i\}$$

$$k = 1, ..., l_i - 2$$

By following the same substitution procedure and using $\sum_{k=1}^{i} sx_k^t \le iN_i^t / l_i$, one can find

$$\Psi_1^t = \max\{0, sx_1^t - Q_i^t, x_i^t - (l_i - 1)N_i^t / l_i\}$$

Thus the receiving capacity of cell i is given by

$$R_i^t = \min\{Q_i^t, N_i^t / l_i - \Psi_1^t\} = \min\{Q_i^t, N_i^t / l_i, N_i^t / l_i - x_1^t + Q_i^t, N_i^t - x_i^t\}$$
$$= \min\{Q_i^t, \ N_i^t / l_i, \ N_i^t - x_i^t\}$$

Notation

The following symbols are used in this paper.

C, C_r, C_S	=	Set of general cells, origins (source cells) and destinations (sink cells);
D_r	=	Total evacuation demand from origin r (veh);
N_i^t	=	Number of vehicles that can present in cell i during t;
Q_i^t	=	Number of vehicles that can flow into/out of cell i during t;

R_i^t	=	Receiving capacity of cell i during interval t (veh);
S_i^t	=	Sending capability of cell i during interval t (veh);
T	=	Required evacuation clearance time (no. of intervals);
d_r^t	=	Evacuation demand from origin r during interval t (veh);
l_i	=	Size of cell i ;
r,s	=	Index of each source cell and sink cell;
x_i^t	=	Number of vehicles in cell i at the beginning of interval t ;
y_{ij}^t	=	Connector flows from cell i to cell j during t ;
$\Gamma(i)$	=	The set of downstream cells to cell i ;
$\Gamma^{-1}(i)$	=	The set of upstream cells to cell i ;
τ	=	Unit time interval (s).

References

1. Alsnih, R., and Stopher, P.R. (2003). "Review of the Procedures Associated with Devising Emergency Evacuation Plans." *Transportation Research Record 1865*, Transportation Research Board, Washington D.C., 89-97.

2. Barrett, B., Ran B., and Pillai, R. (2000). "Developing a Dynamic Traffic Management Modeling Framework for Hurricane Evacuation." *Transportation Research Record 1733*, Transportation Research Board, Washington D.C., 115-121.

3. Daganzo, F.C. (1994). "The Cell Transmission Model: A Dynamic Representation of Highway Traffic Consistent With the Hydrodynamic Theory." *Transportation Research Part B*, 28(4), 269-287.

4.   Daganzo, F.C. (1995). "The Cell Transmission Model. II. Network Traffic." *Transportation Research Part B*, 29(2), 79-93.

5.   Demuth, J.L. (2002). "Countering Terrorism: Lessons Learned From Natural and Technological Disasters." National Academy of Sciences, Washington, D.C.

6.   Franzese, O., and Han, L.D. (2001). "Traffic Modeling Framework for Hurricane Evacuation." Presented at the *80th Transportation Research Board Annual Meeting*, Washington, D.C.

7.   Hobeika, A.G., and Jamei, B. (1985). "MASSVAC: a model for calculating evacuation times under natural disasters." Emergency Planning, Simulations Series 15, 23-28.

8.   Hobeika, A. G., Kim, S., and Beckwith, R. E. (1994). "A decision support system for developing evacuation plans around nuclear power stations." *Interfaces Journal*, 24(5), 22-35.

9.   Hobeika, A.G., and Changykun, K. (1998). "Comparison of Traffic Assignments in Evacuation Modeling." *IEEE Transactions on Engineering Management*, 45(2), 192-198.

10. Jha, M., Moore, K., and Pashaie, B. (2004). "Emergency Evacuation Planning with Microscopic Traffic Simulation." Presented at the *83rd Transportation Research Board Annual Meeting*, Washington, D.C.

11. Li, Y., Ziliaskopoulos A.K. and Waller, S. T. (1999). "Linear Programming Formulations for System Optimum Dynamic Traffic Assignment with Arrival Time-based and Departure time-based Demands." *Transportation Research Record 1667*, Transportation Research Board, Washington D.C., 52-59.

12. Pidd, M., de Silva, F.N., and Eglese, R.W. (1996). "Theory and Methodology: A Simulation Model for Emergency Evacuation." *European Journal of Operational Research*, 90(3), 413-419.

13. Sheffi, Y., Mahmassani, H., and Powell W.B. (1982). "A Transportation Network Evacuation Model" *Transportation Research Part A*, 16(3), 209-218.

14. Theodoulou, G., and Wolshon, B. (2004). "Modeling and Analyses of Freeway Contraflow to Improve Future Evacuations." Presented at the *83rd Transportation Research Board Annual Meeting*, Washington, D.C.

15. Tuydes, H., and Ziliaskopoulos, A. (2004). "Network Re-design to Optimize Evacuation Contraflow." Presented at the *83rd Transportation Research Board Annual Meeting*, Washington, D.C.

16. Urbina, E., and Wolshon, B. (2003). "National review of hurricane evacuation plans and policies: a comparison and contrast of state practices." *Transportation Research Part A*, 37(3), 257–275.

17. Ziliaskopoulos, A., and Lee, S. (1996). "A Cell Transmission Based Assignment-Simulation Model for Integrated Freeway/Surface Street Systems." Presented at the *75th Transportation Research Board Annual Meeting*, Washington, D.C.

18. Ziliaskopoulos, A.K. (2000). "A Linear Programming Model for the Single Destination System Optimum Dynamic Traffic Assignment Problem." *Transportation Science*, 34(1), 37-49.

19. Zou, N., and Yeh, S.T. (2005) "An Simulation-based Emergency Evacuation System for Ocean City, Maryland during Hurricane Attacks." *Transportation Research Record 1922*, Transportation Research Board, Washington D.C., 138-148

20. "Responding to Energy-Related Emergencies." *Oak Ridge National Laboratory Review*, 35(2), 2002, 21-24

21. Town of Ocean City, Maryland, Emergency Operations Plan, December 2002

Table 1. Diverging Proportions for Cells 6 and 7

| Connector	First 3hr 20 min	Last 40 min
6→7: US50 through	0.5	0
6→40: US50 to US113 south	0.5	1
7→8: US50 through	0.8	1
7→24:US50 to MD346	0.2	0

Figure Captions

Figure 1. Graphical Illustration of Cell Connections

Figure 2. Cell connection Diagrams for Test 1

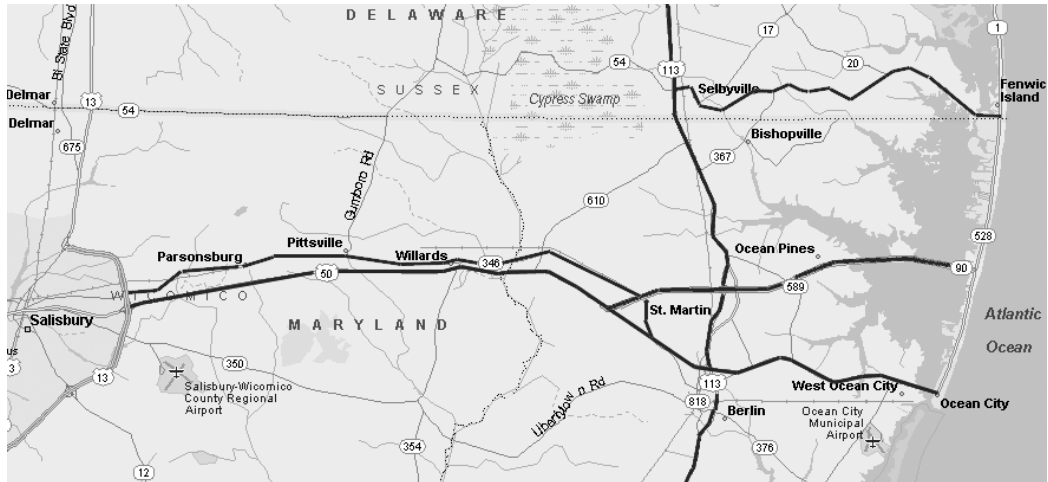Figure 3. Cumulative Arriving Curves for Test 1
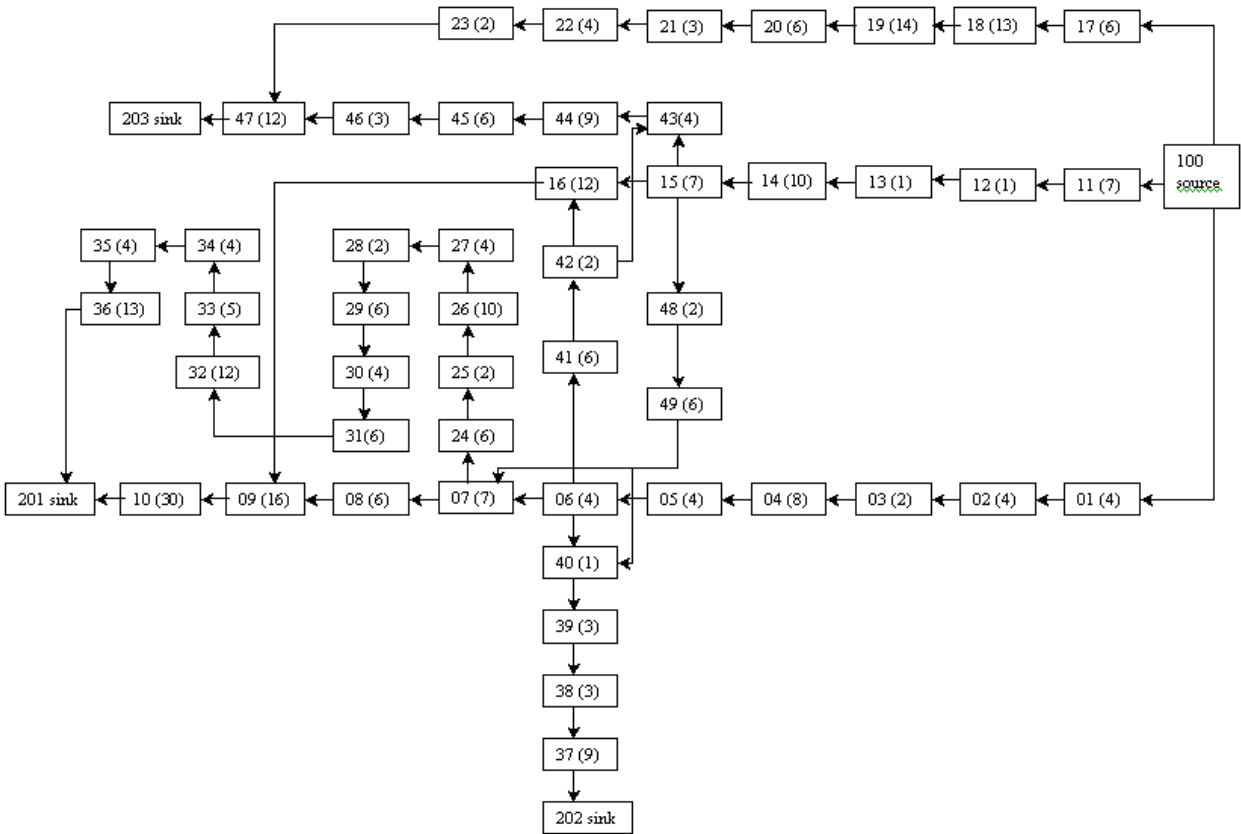
Figure 4. Major Evacuation Network for Ocean City

Figure 5. The Cell Connection Diagram for Ocean City Hurricane Evacuation
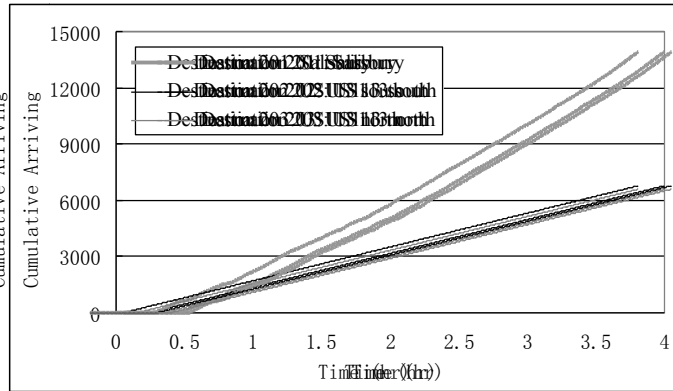
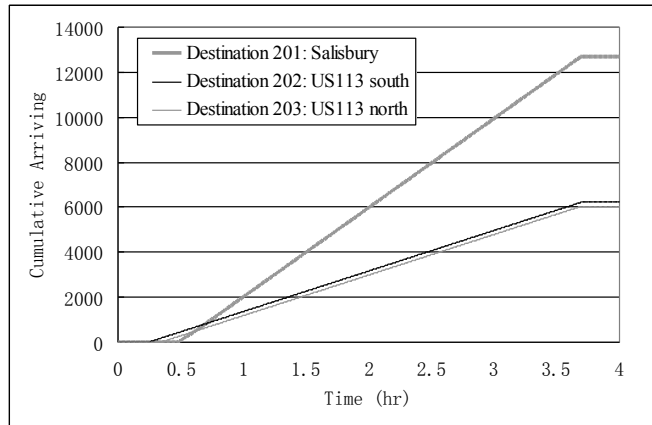Figure 6. Cumulative Arriving Curves for High-Level Optimization

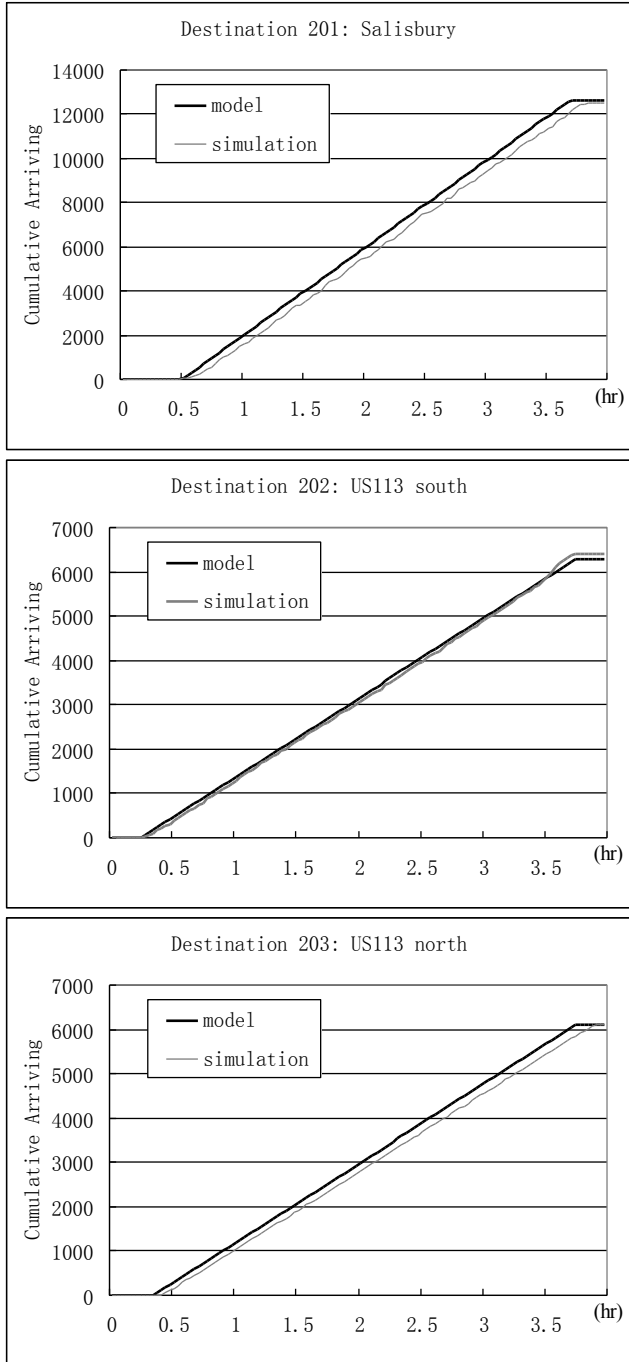Figure 7. Cumulative Arriving Curves for Low-Level Optimization

Figure 8. Comparison of Cumulative Arriving Curves from the Model and Simulation
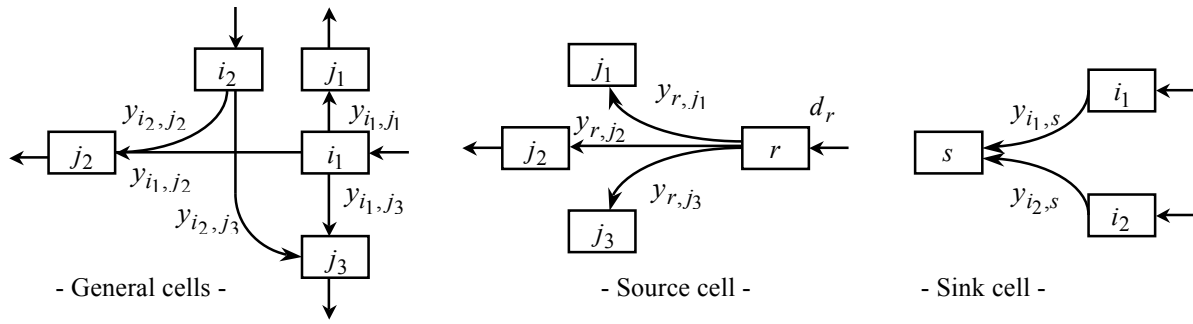
Figure 1. Graphical Illustration of Cell Connections
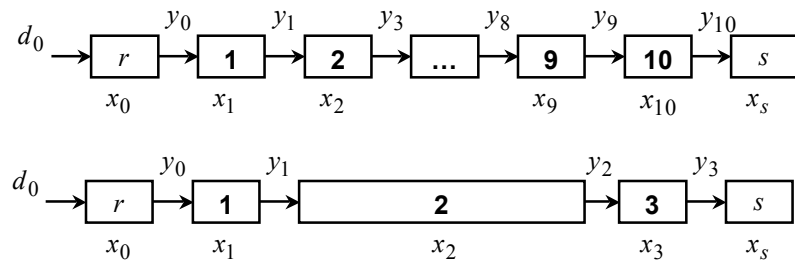
Figure 2. Cell Connection Diagrams for Test 1
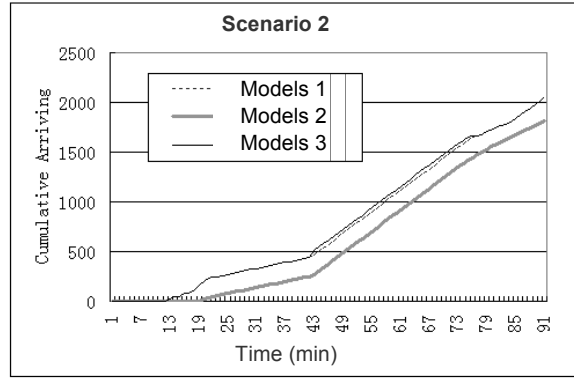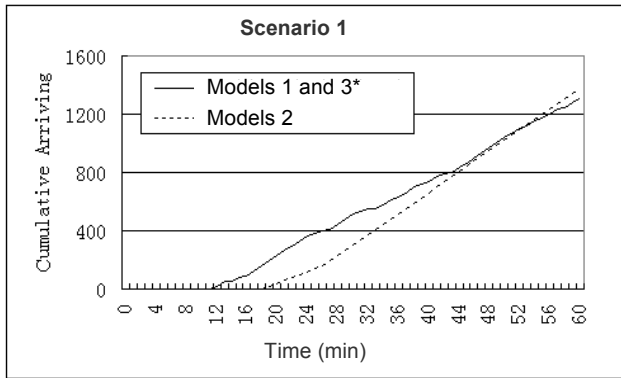
* Models 1 and 3 produce the identical results

Figure 3. Cumulative Arriving Curves for Test 1

Figure 4. Major Evacuation Network for Ocean City

Figure 5. The Cell Connection Diagram for Ocean City Hurricane Evacuation

Figure 6. Cumulative Arriving Curves for the High-Level Optimization

Figure 7. Cumulative Arriving Curves for the Low-Level Optimization

Figure 8. Comparison of Cumulative Arriving Curves

from the Model and Simulation